The PI3K/mTOR inhibitor PF-04691502 induces apoptosis and inhibits microenvironmental signaling in CLL and the Eμ-TCL1 mouse model

Matthew D. Blunt[#1], Matthew J. Carter[#1], Marta Larrayoz[1], Lindsay D Smith, Maria Aguilar-Hernandez[1,2], Kerry L Cox[1], Thomas Tipton[1], Mark Reynolds[1], Sarah Murphy[1], Elizabeth Lemm[1], Samantha Dias[1], Andrew Duncombe[1,3], Jonathan C. Strefford[1], Peter W. M. Johnson[1], Francesco Forconi[1,3,4], Freda K Stevenson[1], Graham Packham[1], Mark S. Cragg[1], Andrew J. Steele[1]

[1] Cancer Sciences Unit, Faculty of Medicine, University of Southampton, Southampton, United Kingdom SO16 6YD

[2] Instituto Nacional de Pediatría Insurgentes Sur 3700-C Col. Insurgentes Cuicuilco C.P. 04530 Mexico

[3] Hematology department, Southampton General Hospital, Southampton, United Kingdom SO16 6YD

[4]Cancer Sciences Unit, Cancer Research UK and NIHR Experimental Cancer Medicine Centres, University of Southampton, Southampton

[#] these authors contributed equally

Running title: Dual PI3K/mTOR inhibition in CLL

Scientific category: Lymphoid neoplasia

Corresponding author: Andrew J. Steele, Cancer Sciences Unit, Somers Building (Mailpoint 824), Southampton General Hospital, Tremona Rd, Southampton SO16 6YD, UK

E-mail: a.steele@soton.ac.uk

Phone: +44(0)2381205170

Fax: +44(0)23805152

Text word count: 3983

Abstract word count: 200

Number of Figures: 7

KEY POINTS:

- PF-04691502 induces potent apoptosis in CLL cells and supresses pro-survival anti-IgM signaling and CXCL12-induced migration.
- PF-04691502 displays powerful anti-tumor effects *in vivo* in the Eμ-TCL1 mouse model

ABSTRACT

Current treatment strategies for CLL involve a combination of conventional chemotherapeutics, monoclonal antibodies and targeted signaling inhibitors. However, CLL remains largely incurable with drug resistance and treatment relapse a common occurrence; leading to the search for novel treatments. mTOR specific inhibitors have been previously assessed but their efficacy is limited due to a positive feedback loop via mTORC2, resulting in activation of pro-survival signaling. Here we show that the dual PI3K/mTOR inhibitor PF-04691502 does not induce an mTORC2 positive feedback loop similar to other PI3K inhibitors but does induce substantial anti-tumor effects. PF-04691502 significantly reduced survival coincident with the induction of Noxa and Puma, independently of IGHV mutational status, CD38 and ZAP-70 expression. PF-04691502 inhibited both anti-IgM induced signaling and overcame stroma-induced survival signals as well as migratory stimuli from CXCL12. Equivalent *in vitro* activity was seen in the Eμ-TCL-1 murine model of CLL. *In vivo*, PF-04691502 treatment of tumor-bearing animals resulted in a transient lymphocytosis, followed by a clear reduction in tumor in the blood, bone marrow, spleen and lymph nodes. These data indicate that PF-04691502 or other dual PI3K/mTOR inhibitors in development may prove efficacious for the treatment of CLL, increasing our armamentarium to successfully manage this disease.

INTRODUCTION

Chronic Lymphocytic Leukemia (CLL) is characterized by the accumulation of $CD5^{+}CD19^{+}$ cells in the peripheral blood, lymph nodes and bone marrow. Several prognostic markers are associated with progressive disease; these include unmutated immunoglobulin heavy chain variable regions (IGHV) and high expression of CD38 and ZAP-70.[1] Current treatment strategies involve the combination of fludarabine, cyclophosphamide and rituximab,[2] however CLL largely remains incurable with drug resistance and treatment relapse a common occurrence.[3]

Recently, inhibitors targeting key signaling molecules such as BTK (ibrutinib) and PI3K (idelalisib) have been approved,[4,5] due to exceptional clinical responses.[6-11] In this regard, the PI3K/mTOR pathway is particularly attractive because it is activated upon ligation of various chemokine and cytokine receptors expressed by CLL cells as well as following B cell receptor (BCR) engagement.[12] Class 1 PI3Ks are divided into Class 1A (PI3Kα, PI3Kβ and PI3Kδ) and Class 1B (PI3Kγ) isoforms. The expression of PI3Kδ and PI3Kγ is largely restricted to leukocytes, whilst the expression of PI3Kα and PI3Kβ is ubiquitous. PI3Kδ and PI3Kγ have crucial roles in a plethora of leukocyte functions including proliferation, antibody secretion, survival, migration[13] and ROS generation.[14] Functional redundancy between PI3K isoforms is evident and supported by the fact that multiple isoforms require inhibition to fully reverse the neutrophil survival induced by GM-CSF.[15] PI3K exists in a complex signaling network with multiple partners including those regulating mTOR. mTOR-complex-1 (mTORC1) is a serine/threonine kinase activated downstream of PI3K which controls protein translation, growth and proliferation in part via modulation of S6 ribosomal subunit activity.[16] In contrast, mTOR complex 2 (mTORC2) phosphorylates AKT^{S473} and is required for maximal activation of AKT[16] (Supplementary Figure 1A and B).

PI3K signaling is known to be overactive in CLL,[17] with patients with unmutated IGHV having increased PI3K gene expression compared to patients with mutated IGHV.[18] The PI3Kδ selective inhibitor Idelalisib has been approved by the FDA to treat CLL patients with relapsed disease in combination with rituximab.[4] Idelalisib inhibits chemokine- and BCR-induced signaling and sensitizes CLL cells to standard genotoxic agents.[19-21] In patients, Idelalisib has a dual mechanism of action: 1) directly reducing CLL cell viability; and 2) disrupting stromal cell interactions and releasing CLL cells from their protective microenvironments into the blood, where they are more susceptible to chemotherapy-induced apoptosis. However single isoform inhibitors against PI3Kα/β/δ and pan-class1 PI3K inhibitors in CLL cells have all been reported to induce apoptosis.[22,23] Pharmacological inhibition of mTOR

induces cell cycle arrest and apoptosis in CLL cells,[24-26] however prolonged inhibition of mTOR is known to disrupt negative feedback loops and cause increased AKT^{S473} activation in other malignancies.[27,28]

Given the important role of both PI3K and mTOR in CLL cell survival, the dual pharmacological inhibition of both Class 1 PI3K and mTOR signaling may offer new therapeutic potential, with the possibility of deeper remissions or as an alternative following resistance to idelalisib. PF-04691502 is a potent selective dual Class 1 pan-PI3K/mTOR inhibitor[29] shown to inhibit tumor growth and to promote apoptosis in solid tumors.[29-33] PF-04691502 inhibits (IC_{50}) PI3Kδ 1.6nM(Ki), PI3Kα 1.8nM(Ki), PI3Kγ 1.9nM(Ki), PI3Kβ 2.1nM(Ki) and in cells has shown IC_{50} values of 3.8nM and 7.5nM for P-AKT^{S473} and P-AKT^{T308}, respectively.[29] During phase I clinical trials, PF-04691502 was shown to have a similar safety profile to other PI3K inhibitors.[34]

In this study we showed in primary CLL cells that PF-04691502 induced caspase-dependent apoptosis. In contrast, little effect on the viability of normal B and T lymphocytes was evident. BCR and CXCR4 stimulated signaling was inhibited by PF-04691502 and chemokine mediated motility was potently reduced. Similarly impressive anti-tumor effects were seen with the Eμ-TCL1 murine CLL-like cells *in vitro* and *in vivo*. Together these data indicate that concomitant targeting of mTOR and PI3K is a powerful approach for treating CLL.

MATERIALS AND METHODS

Patients and cells

Diagnosis of CLL was according to the IWCLL-NCI 2008 criteria.[35] Forty-nine CLL isolates were studied following informed written consent in accordance with ethics committee approvals under the declaration of Helsinki (reference 228/02/t) (Supplementary Table 1). Procedures for the isolation of malignant cells and the determination of their purity have been described previously.[36] All isolates contained >90% $CD19^+CD5^+$ cells. Normal B and T lymphocytes from peripheral blood were taken from healthy age-matched controls as previously described.[37]

Reagents

Tissue culture materials were from life technologies (Paisley, UK). ZVAD.fmk was from Enzo life sciences (Exeter, UK). PF-04691502 was provided by Pfizer Inc. and purchased from Selleckchem for *in vivo* studies (Houston USA). Idelalisib, BYL719, Everolimus, GSK2636771, and AS-605240 and were from Selleckchem (Houston, USA). Annexin-V was from the Southampton CR-UK core proteomics

facility. Anti-IgM was from Cambridge Bioscience (Cambridge, UK) and CXCL12 from Miltenyi (Bisley, UK). HFFF2 cells were a kind gift from Prof. Thomas (University of Southampton).

Cell culture and protein extraction

CLL cell culture and protein extraction for immunoblotting were as previously described.[38,39] Soluble anti-IgM was used at 20µg/ml, bead bound immobilised anti-IgM was added at 2:1 ratio, bead:CLL cell. Densitometry of immunoblots are depicted in Supplementary Figures 6 and 7.

Gel electrophoresis and Immunoblotting

Proteins were separated on 12% polyacrylamide gels (LifeTechnologies, Paisley Scotland), transferred to nitrocellulose membranes (GE Healthcare, Buckinghamshire, UK) and probed with antibodies listed in Supplementary Table 2. Bands were detected by incubation with HRP-linked secondary antibodies (Dako), enhanced chemiluminescence reagents (Thermo Scientific, Rockford, IL) and visualised using the ChemiDoc-It imaging system (UVP). Band intensities were quantified using ImageJ.

Viability assays

CLL cells were treated with PF-04691502 for 24h and viability assessed by Annexin V-FITC and propidium iodide (PI) negativity as previously described.[39] Fifty percent inhibitory concentration values (IC_{50}) were measured using CalcuSyn software (Biosoft, Cambridge). Peripheral blood mononuclear cells from normal donors were plated at 1×10^6cells/ml, treated with PF-04691502 for 24h and normal T and B cells labelled with APC conjugated anti-CD3 or anti-CD19 respectively, in combination with Annexin V-FITC/PI.[37]

Eµ-TCL1 experiments

In vitro analysis using Eµ-TCL1 cells were performed at 2.5 $x10^6$ cells/ml. For *in vivo* experiments, $1x10^7$ Eµ-TCL1 leukemia cells were given by intra-peritoneal injection to congenic, age-matched female C57BL/6 mice, n= 7 per group. Leukemic burden was assessed by tail bleeding, and monitoring total lymphocyte counts and the percentage of $CD5^+B220^{lo}$ cells by flow cytometry. PF-04691502 was administered in 0.5% methylcellulose by oral gavage at either 5 or 10mg/kg/day. Animals were sacrificed and organs harvested for further analysis. Total organ tumor burden was calculated by $CD5^+B220^{lo}$ flow cytometry using quanti-bright counting beads (Life Technologies, UK).

RESULTS

mTOR inhibition of CLL cells augments AKT^{S473} signaling

Previous studies in other tumor systems have shown that inhibition of mTOR with everolimus/rapamycin results in augmentation of the mTORC2 target, AKT^{S473}.[27,28] Here we show that this also occurs in CLL cells both in resting conditions and more effectively following BCR engagement with soluble anti-IgM antibodies (Figure 1A and 1B) with the expected effects on the mTOR target phosphorylated (p)S6 kinase (pS6K) (Figure 1C). In contrast, the dual PI3K/mTOR inhibitor PF-04691502 does not induce hyperphosphorylation of AKT^{S473} and inhibits the pathway as shown with other PI3K inhibitors (Supplementary Figure 1C). Phosphorylated-S6K was completely abrogated with PF-04691502, whilst phosphorylated S6 ribosomal protein (pS6$^{S235/236}$) is regulated by both the MAPK and PI3K/mTOR signalling pathways and was therefore only partially affected by both everolimus and PF-04691502 (Figure 1D). AKT is also phosphorylated at AKT^{T308} in a PI3K-dependent manner by PDK and was not significantly augmented by everolimus treatment before or after anti-IgM treatment. However, PF-04691502 completely abrogated AKT^{T308} phosphorylation (Figure 1E). Together these data indicate that the same negative feedback loop involving mTORC2 is in operation in CLL cells but is circumvented by PF-04691502.

PF-04691502 reduces cell viability in CLL cells independently of prognostic markers

CLL samples were treated with PF-04691502 and viability assessed using annexin-V/PI staining (Supplementary Figure 2A). PF-04691502 reduced viability of CLL cells after 24, 48 and 72h hours (Figure 2A & 2B) with a mean IC_{50} of 0.96μM (median 0.65μM), 0.32μM and 0.25μM, respectively. The same CLL samples treated with idelalisib did not reach its IC_{50} value up to 40μM (Figure 2A) in agreement with the literature.[19,20] Normal B and T cells from age-matched controls were largely unaffected by PF-04691502 over a similar dose range. No significant differences in mean IC_{50} values for PF-04691502 were observed between unmutated (U-CLL) and mutated (M-CLL) IGHV genes (Figure 2B), high and low ZAP-70 (>30%) (Figure 2C) or CD38 expression (>30%) (Figure 2D). However a trend for lower IC_{50} values was observed in U-CLL compared to M-CLL. Furthermore, three CLL samples with 17p del (2/3 samples >70% 17p del by FISH) were as susceptible to PF-04691502-induced death as wildtype samples (Supplementary Figure 2B), indicating that PF-04691502 may also have activity independent of 17p del status.

Combination of isoform specific PI3K inhibitors and an mTOR inhibitor mimic PF-04691502

PF-04691502 reduced viability of CLL cells to a greater extent compared to idelalisib. Therefore, we sought to determine whether we could replicate its efficacy using a combination of isoform-specific

PI3K inhibitors including BYL719 (PI3Kα inhibitor), GSK2636771 (PI3Kβ inhibitor), idelalisib (PI3Kδ inhibitor), AS-605240 (PI3Kγ inhibitor) in combination with the mTOR inhibitor everolimus (mTORC1 inhibitor). Each inhibitor alone (1μM) reduced viability by no more than ~10% (Supplementary Figure 2C). This was in contrast to PF-04691502, which at the same concentration reduced CLL cell viability by >50%. The combination of all five selective inhibitors at 1μM significantly reduced CLL cell viability more than any of the inhibitors alone, albeit significantly less than PF-04691502 (p=0.004, n=11). Finally we showed that a combination of idelalisib with everolimus was significantly more efficacious than either agent alone (p=0.02 and p=0.01) (Supplementary Figure 2D) but significantly less than PF-04691502 (p=0.03). Together these data suggests that PF-04691502 likely achieves its robust killing effects through simultaneous inhibition of mTORC1, mTORC2 and PI3Kδ.

PF-04691502 induces apoptosis in a caspase-dependent mechanism

To determine the mechanism of death induced by PF-04691502, we first investigated expression of key pro-apoptotic BH3-only proteins Noxa, Puma, Bad, Bim and Bax, and anti-apoptotic Bcl-2 family proteins Mcl-1 and Bcl-2 which regulate apoptosis within CLL cells. Incubation with PF-04691502 (0.31-1.25μM) induced Noxa and Puma expression (protein and mRNA) in a dose-dependent manner (Figure 3A and data not shown). No significant changes were observed for Bim, Bad, Bcl-2 or Mcl-1 (data not shown). Basal $pAKT^{S473}$ and $pS6K^{T389}$ were inhibited by PF-04691502 as expected. In response to pro-apoptotic stimuli, Bax undergoes a conformational change and subsequently becomes inserted into the outer mitochondrial membrane where it facilitates cytochrome c release and subsequent apoptosis. Using the conformational change specific 6A7 antibody[37] we showed that CLL cells incubated with PF-04691502 produced a marked increase in the active, mitochondrially-resident conformation of Bax (Figure 3B). Furthermore treatment of CLL cells with PF-04691502 (0.31-5μM) for 18 hours induced caspase-3 cleavage and subsequent appearance of the p85 cleaved sub-fragment of PARP (Figure 3C). To confirm PF-04691502 induced apoptosis of CLL cells in a caspase-dependent manner, we treated cells with the pan-caspase inhibitor ZVAD.fmk. ZVAD.fmk significantly prevented the PF-04691502 induced decrease in cell viability even at the highest concentrations of PF-04691502 (20μM) ($p<0.001$, n=7) (Figure 3D).

PF-04691502 reduced viability of CLL cells in co-culture with stromal cells

CLL cells are known to receive key survival signals from stromal cells in the bone marrow and lymph nodes, reducing CLL apoptosis and promoting drug resistance.[12] Therefore, we investigated the effect of PF-04691502 upon CLL cells co-cultured with human stromal fibroblast cells (HFFF2) which we have observed can provide anti-apoptotic signaling to CLL cells (manuscript in preparation). PF-04691502

significantly inhibited signaling induced by HFFF2 (Supplementary Figure 3A) and reduced CLL cell viability (p=0.016), thus showing its ability to overcome stromal support (Figure 3E). To preclude that its activity was due to a direct cytotoxic effect on the fibroblasts (Supplementary Figure 3B) we also performed "wash-out" experiments where PF-04691502 was added to the CLL cells for 1h and washed off prior to addition to the HFFF2 cells. Cell viability was still significantly reduced by PF-04691502 (p=0.016) and downstream signaling inhibited in this setting (Figure 3F, Supplementary Figure 3C).

Dual PI3K/mTOR inhibition decreases pro-survival BCR signaling

Ligation of the CLL BCR by antigen/autoantigen is thought to primarily occur in the lymph nodes, acting to enhance CLL survival and resistance to chemotherapy.[40] Antigen in lymph nodes may be present in both soluble and membrane bound forms. Therefore, we utilised both soluble and bead-immobilised anti-IgM[41] to investigate the effect of PF-04691502 (2.5-2500nM) on BCR signaling. Analysis of downstream signaling showed that both the soluble (Figure 4A) and bead-immobilised (Figure 4B) anti-IgM induced strong activation of pAKT$^{S473/T308}$, pERK$^{T202/Y204}$, pS6K^{T389} and pS6$^{S235/236}$ ribosomal subunit. PF-04691502 significantly inhibited pAKT$^{S473/T308}$ and pS6K^{T389} in CLL samples following both soluble and immobilised anti-IgM treatment and at concentrations below maximum achievable plasma drug concentrations (100-200nM).[34] pERK$^{T202/Y204}$ and pS6$^{S235/236}$ were significantly inhibited by PF-04691502 following soluble (Figure 4A) but not immobilised (Figure 4B) anti-IgM treatment. These data indicate that PF-04691502 inhibits PDK1-mediated pAKT^{T308}, mTORC1-induced pS6K^{T389} and mTORC2-mediated pAKT^{S473} activation. Furthermore activation of these BCR-signals with immobilised anti-IgM beads strongly protects CLL cells from apoptosis as indicated by a decrease in cleaved caspase-3 and PARP compared to the control, but was reversed upon treatment with PF-04691502 (Supplementary Figure 4A).

PF-04691502 inhibits CXCL12 induced signaling and subsequent migration

In vivo, CXCL12 signaling enables CLL cells to enter and become retained within protective lymph node microenvironments.[12] Therefore, disruption of CXCL12/CXCR4 signaling provides an attractive therapeutic target.[12] Here, CLL cells treated with CXCL12 (200ng/ml) for 10 minutes showed increased pAKT^{S473}, pS6K^{T389} and pS6$^{S235/236}$ which was reversed following treatment with PF-04691502 (Figure 5A). In contrast, pERK$^{T202/Y204}$ was not affected by PF-04691502 pre-treatment, potentially due to downstream signalling from Syk/Ras being unaffected by PF-04691502. Next, we determined the effect of PF-04691502 on CLL motility in an *in vitro* transwell migration assay. Treatment of CLL cells with PF-04691502 showed no significant effect on basal CLL motility, however CXCL12-induced CLL motility was significantly abrogated following pre-treatment with PF-04691502 for only 30 minutes

(p=0.02 and p=0.025 at 1.25 and 2.5μM, respectively) (Figure 5B) and was not dependent on reduced expression of CXCR4 (Supplementary Figure 4B). These data indicate that PF-04691502 inhibits CXCL12 signalling and subsequent migration, which has potential importance for CLL cells accessing the protective lymph node microenvironment *in vivo*.

PF-04691502 has efficacy in murine Eμ-TCL1 CLL cells *ex vivo*

Next, we examined whether PF-04691502 displayed activity against murine Eμ-TCL1 tumor cells, isolated and cultured *ex-vivo*. Eμ-TCL1 tumor cells were isolated from the spleens of tumor-bearing mice and then treated with anti-IgM or CXCL12 in the presence or absence of PF-04691502 and the effects on downstream signaling investigated by immunoblotting. PF-04691502 substantially blocked signaling induced by both stimuli, reducing $pAKT^{T308}$, $pAKT^{S473}$, $pS6K^{T389}$ and $pS6^{S235/236}$ to below background levels, with lesser effects on $pERK^{T202/Y204}$ at 2.5-25nM PF-04691502 (Figure 6A and 6B). These effects translated into an ability of PF-04691502 to efficiently kill Eμ-TCL1 tumor cells (n=8 different tumors) (Figure 6C) and inhibit migration towards CXCL12 (Figure 6D). These data recapitulated those seen with primary human CLL cells above.

***In vivo* efficacy of PF-04691502**

Finally, we explored the activity of PF-04691502 *in vivo*. Cohorts of mice were inoculated with Eμ-TCL1 tumor cells and when tumor was visible in the blood (approximately 21 days), mice were randomised to receive 5 or 10mg/kg/day PF-04691502 or vehicle control by oral gavage and the leukemic burden in the blood was monitored over the following 14 days (Figure 7A). After receiving the drug a small but significant lymphocytosis was observed which persisted for approximately 4-7 days. Subsequently, PF-04691502 elicited a marked reduction in leukemic burden compared to the vehicle control (p=0.0001), indicating a profound anti-tumor effect. Both drug doses demonstrated the same efficacy, indicating that the minimum effective dose was achieved. Fourteen days post treatment vehicle-recipient animals exhibited a terminal disease and were sacrificed alongside mice receiving 10mg/kg/day PF-04691502 and the effects of the drug on multiple tissues including the spleen, lymph nodes and bone marrow (Figure 7B-D) determined. Mice receiving 5 mg/kg/day were maintained on drug for survival experiments. Visual assessment and weighing of the spleen illustrated the ability of the drug to prevent tumor expansion at this site (Figure 7B and 7C); which was confirmed by enumerating the number of tumor cells (Figure 7D). In fact, no increase in splenic mass was observed compared to normal healthy C57BL/6 mice, whereas vehicle-treated mice exhibited a 4-8 fold increase in splenic mass, alongside a tumor cell count an order of magnitude higher than PF-04691502 treated mice. Next, we examined the macroscopic appearance of the spleen using Hematoxylin and eosin

(H&E) staining (Supplementary Figure 5A). These images indicate that the Eμ-TCL1 leukemias destroy the typical splenic architecture, whereas this was largely prevented by PF-04691502 treatment. In addition to the spleen, we also observed similar effects of the drug reducing tumor expansion in the lymph nodes and bone-marrow (Figure 7D). Cumulatively, these effects significantly enhanced survival in 5 mg/kg/day-recipient animals (p=<0.0001) (Supplementary Figure 5B). Furthermore, mice showed a small but significant reduction in normal B-cell number but no significant reduction in normal T-cell number (data not shown). These data indicate that PF-04691502 has substantial efficacy *in vivo,* warranting further investigation of dual PI3K/mTOR inhibitors for the treatment of CLL.

DISCUSSION

Treatment of CLL patients with ibrutinib and idelalisib have produced impressive clinical responses, however the agents are not curative and only suppress the disease. Therefore, identifying an agent that can purge CLL cells from the protective lymph node and bone marrow niches in combination with substantive tumor toxicity may prove essential for an eventual cure. Our results showed that PF-04691502 inhibited BCR and CXCL12 induced signaling, resulting in caspase-dependent apoptosis of CLL cells *in vitro* at nanomolar concentrations, whilst treatment of normal B and T cells resulted in little to no death. Caspase-dependency was confirmed with the pan-caspase inhibitor ZVAD.fmk and was preceded by the pro-apoptotic conformational change in Bax. Bax activation correlated with the induction of the BH3-only Bcl-2 family members Noxa and Puma suggesting activation of the intrinsic apoptotic pathway. However, since 17p del cases displayed equivalent sensitivity to PF-04691502 as wildtype samples, the pathway leading to Noxa and Puma induction after PF-04691502 treatment may be TP53-independent. The mechanism behind the Noxa and Puma induction is currently unknown and is the subject of our ongoing studies. PF-04691502 induced apoptosis independently of known prognostic markers, which is consistent with findings with idelalisib in CLL.[19] However, an intriguing finding was the enhanced apoptotic potency of PF-04691502 in comparison to idelalisib.[19,42] This increased cytotoxicity against CLL cells by PF-04691502 may be due to inhibition of more than one PI3K isoform or more likely due to the co-inhibition of PI3K and mTORC1/2. Evidence in mantle cell lymphoma to support this has shown constitutive PI3Kα signaling limits the efficacy of PI3Kδ selective inhibitors.[43] Functional redundancy between PI3K isoforms in the survival of neutrophils has previously been shown,[15] therefore it may be theorized that in CLL cells other PI3K isoforms may compensate for the selective inhibition of PI3Kδ with idelalisib, resulting in lower levels of cytotoxicity with this drug. However the γ/δ inhibitor IPI-145 did not increase CLL cell apoptosis more than idelalisib in vitro.[44] In contrast, the dual PI3Kα/γ inhibitor PIK90 and the pan-PI3K inhibitor NVP-BKM120 (Buparlisib) induce substantially more CLL cell apoptosis,[23,45] than single isoform inhibitors.[19]

The potential caveat to inhibition of more than a single PI3K isoform is the possibility of greater toxicity to normal tissues. However, a number of pan-PI3K inhibitors and dual PI3K/mTOR inhibitors are currently progressing through clinical trials for various malignancies with promising results.[46] Interestingly, long-term PI3Kα inhibition was not detrimental to mice and in fact protected against a reduction in insulin sensitivity, glucose tolerance and fat accumulation.[47] During our study we combined inhibitors that targeted specific isoforms of PI3K and mTOR; replicating our findings with PF-04691502. Although combining the PI3Kα/β/δ/γ inhibitors or idelalisib with the mTOR inhibitor everolimus induced substantial apoptosis, PF-04691502 alone still induced significantly more. This may be because everolimus inhibits predominately mTORC1, whilst PF-04691502 inhibits both mTORC1 and mTORC2, which is essential to inhibit the positive feedback and subsequent phosphorylation of AKT^{S473}. However, these data suggest that an mTORC1 inhibitor, and maybe more importantly a dual mTORC1/2 inhibitor, in combination with idelalisib may be more therapeutically beneficial in the treatment of CLL than PI3K inhibition alone.

Ligation of the BCR occurs primarily in the protective lymph node microenvironment[48] and is thought to be crucial for survival of the malignant clone.[40] Furthermore, CXCL12 induces migration of the CLL cells from the periphery into the lymph node promoting their retention within protective microenvironments.[12] CXCL12/CXCR4 signaling has previously been shown to inhibit spontaneous cell death and chemotherapy-induced apoptosis.[49] Therefore, our finding that PF-04691502 could overcome pro-survival anti-IgM induced signaling and substantially inhibit CXCL12 signaling and subsequent CLL migration is of clear importance. This is also in agreement with what has been described for idelalisib.[20] These results indicate that PF-04691502 may have similar clinical characteristics to other kinase inhibitors, where the inhibition of BTK, PI3Kδ or SYK results in reduced interaction of CLL cells with its protective microenvironments, re-distribution of the tumor cells from tissues to the blood and some cellular toxicity.[19,50] This resulted in clinical activity whereby patients undergo rapid lymph node shrinkage and lymphocytosis within weeks of treatment initiation.[7,11,20] Due to the relatively low toxicity of these agents alone on CLL cells, combining them with Bcl-2 antagonists (ABT-199) has been proposed. However, given the trend for greater Mcl-1 expression in CLL patient lymph nodes,[51] which is regulated by microenvironmental factors through PI3K, PI3K inhibition may have greater efficacy. This raises the question as to whether targets downstream of PI3K, such as AKT, are equally tractable. However, current data suggest not, as CLL cells treated with AKT inhibitors (MK2206 and AZD5363) required concentrations in excess of 10μM to elicit relatively small amounts of apoptosis and clinical trials have stopped recruiting (NCT01369849).

Tumor cell redistribution was also evident in the Eμ-TCL1 model with a transient lymphocytosis seen in the blood concomitant with reduced tumor load in the secondary lymphoid organs and bone marrow upon PF-04691502 treatment. Such lymphocytosis is likely a consequence of reduced chemokine receptor expression or signal inhibition. Interestingly, although PF-04691502 treatment prevented accumulation of tumor in the spleen and caused protection of the global splenic architecture, tumor was still evident, even in the presence of PF-04691502. Therefore, these tumor deposits likely reflect treatment-resistant reservoirs, which require additional interventions with other treatment modalities. This is the basis for our on-going studies.

The results from this study show that simultaneous inhibition of all four class 1 PI3K isoforms in combination with the inhibition of mTOR kills CLL cells more potently than selective PI3Kδ inhibition alone. The data generated with systems mimicking ongoing BCR stimulation and stromal support indicates its ability to overcome protective microenvironment signalling *in vivo*. These results are supported by *in vivo* experimentation using the Eμ-TCL1 mouse model that further indicates that PF-04691502 may prove therapeutically useful for the treatment of CLL. Further studies are now required to investigate its key modes of action and explore its utility in combination with other treatment modalities.

Acknowledgements: We thank Pfizer Inc. for providing pure substance for this study (PF-04691502), Leukaemia and Lymphoma Research (12044) and Kay Kendall (KKL687) for supporting this work, the patients for supplying tissue and the infrastructure support from a CR-UK centre grant (C34999/A18087). We thank Dr Duriez for the provision of Annexin V-FITC. We would like to thank Dr Egle, Dr Pekarsky and Professor Croce for the provision of the Eμ-TCL-1 mouse model and Prof Thomas for the HFFF2 cells. Finally, we thank Mr Tracy and Mrs Henderson for biobanking and characterisation of the CLL samples used in this study (LLR grant 12021, ECMC C24563/A15581) and Dr Gobessi and Prof. Efremov for advice on the use of the Eμ-Tcl-1 model.

Author contributions: MDB, MJC, JCS, MSC and AJS designed research and wrote the manuscript. MDB, MJC ML, LDS, MH, KLC, TT, MR, LM, SD and SM performed research and analyzed data. FF obtained consent from patients, blood samples and collated and analysed clinical data. AD provided patients and clinical data. FS, PWMJ, GP provided critical review, suggested experiments and edited the paper.

Conflict of interests: The authors state that there are no conflicts of interest.

References

1. Kay NE, O'Brien SM, Pettitt AR, Stilgenbauer S. The role of prognostic factors in assessing 'high-risk' subgroups of patients with chronic lymphocytic leukemia. *Leukemia*. 2007;21(9):1885-1891.
2. Hallek M. Chronic lymphocytic leukemia: 2013 update on diagnosis, risk stratification and treatment. *Am J Hematol*. 2013;88(9):803-816.
3. Pleyer L, Egle A, Hartmann TN, Greil R. Molecular and cellular mechanisms of CLL: novel therapeutic approaches. *Nat Rev Clin Oncol*. 2009;6(7):405-418.
4. Markham A. Idelalisib: first global approval. *Drugs*. 2014;74(14):1701-1707.
5. Cameron F, Sanford M. Ibrutinib: first global approval. *Drugs*. 2014;74(2):263-271.
6. Brown JR, Byrd JC, Coutre SE, et al. Idelalisib, an inhibitor of phosphatidylinositol 3-kinase p110delta, for relapsed/refractory chronic lymphocytic leukemia. *Blood*. 2014;123(22):3390-3397.
7. Byrd JC, Furman RR, Coutre SE, et al. Targeting BTK with ibrutinib in relapsed chronic lymphocytic leukemia. *N Engl J Med*. 2013;369(1):32-42.
8. Davids MS, Brown JR. Targeting the B cell receptor pathway in chronic lymphocytic leukemia. *Leuk Lymphoma*. 2012;53(12):2362-2370.
9. Byrd JC, Brown JR, O'Brien S, et al. Ibrutinib versus ofatumumab in previously treated chronic lymphoid leukemia. *N Engl J Med*. 2014;371(3):213-223.
10. Furman RR, Sharman JP, Coutre SE, et al. Idelalisib and rituximab in relapsed chronic lymphocytic leukemia. *N Engl J Med*. 2014;370(11):997-1007.
11. Friedberg JW, Sharman J, Sweetenham J, et al. Inhibition of Syk with fostamatinib disodium has significant clinical activity in non-Hodgkin lymphoma and chronic lymphocytic leukemia. *Blood*. 2010;115(13):2578-2585.
12. Burger JA, Gribben JG. The microenvironment in chronic lymphocytic leukemia (CLL) and other B cell malignancies: insight into disease biology and new targeted therapies. *Semin Cancer Biol*. 2014;24:71-81.
13. Okkenhaug K. Signaling by the phosphoinositide 3-kinase family in immune cells. *Annu Rev Immunol*. 2013;31:675-704.
14. Kulkarni S, Sitaru C, Jakus Z, et al. PI3Kbeta plays a critical role in neutrophil activation by immune complexes. *Sci Signal*. 2011;4(168):ra23.
15. Juss JK, Hayhoe RP, Owen CE, et al. Functional redundancy of class I phosphoinositide 3-kinase (PI3K) isoforms in signaling growth factor-mediated human neutrophil survival. *PLoS One*. 2012;7(9):e45933.
16. Laplante M, Sabatini DM. mTOR signaling in growth control and disease. *Cell*. 2012;149(2):274-293.
17. Ringshausen I, Schneller F, Bogner C, et al. Constitutively activated phosphatidylinositol-3 kinase (PI-3K) is involved in the defect of apoptosis in B-CLL: association with protein kinase Cdelta. *Blood*. 2002;100(10):3741-3748.
18. Kienle D, Benner A, Krober A, et al. Distinct gene expression patterns in chronic lymphocytic leukemia defined by usage of specific VH genes. *Blood*. 2006;107(5):2090-2093.
19. Herman SE, Gordon AL, Wagner AJ, et al. Phosphatidylinositol 3-kinase-delta inhibitor CAL-101 shows promising preclinical activity in chronic lymphocytic leukemia by antagonizing intrinsic and extrinsic cellular survival signals. *Blood*. 2010;116(12):2078-2088.
20. Hoellenriegel J, Meadows SA, Sivina M, et al. The phosphoinositide 3'-kinase delta inhibitor, CAL-101, inhibits B-cell receptor signaling and chemokine networks in chronic lymphocytic leukemia. *Blood*. 2011;118(13):3603-3612.

21. Lannutti BJ, Meadows SA, Herman SE, et al. CAL-101, a p110delta selective phosphatidylinositol-3-kinase inhibitor for the treatment of B-cell malignancies, inhibits PI3K signaling and cellular viability. *Blood*. 2011;117(2):591-594.
22. de Frias M, Iglesias-Serret D, Cosialls AM, et al. Isoform-selective phosphoinositide 3-kinase inhibitors induce apoptosis in chronic lymphocytic leukaemia cells. *Br J Haematol*. 2010;150(1):108-111.
23. Niedermeier M, Hennessy BT, Knight ZA, et al. Isoform-selective phosphoinositide 3'-kinase inhibitors inhibit CXCR4 signaling and overcome stromal cell-mediated drug resistance in chronic lymphocytic leukemia: a novel therapeutic approach. *Blood*. 2009;113(22):5549-5557.
24. Decker T, Hipp S, Ringshausen I, et al. Rapamycin-induced G1 arrest in cycling B-CLL cells is associated with reduced expression of cyclin D3, cyclin E, cyclin A, and survivin. *Blood*. 2003;101(1):278-285.
25. Hayun R, Okun E, Berrebi A, et al. Rapamycin and curcumin induce apoptosis in primary resting B chronic lymphocytic leukemia cells. *Leuk Lymphoma*. 2009;50(4):625-632.
26. Aleskog A, Norberg M, Nygren P, et al. Rapamycin shows anticancer activity in primary chronic lymphocytic leukemia cells in vitro, as single agent and in drug combination. *Leuk Lymphoma*. 2008;49(12):2333-2343.
27. O'Reilly KE, Rojo F, She QB, et al. mTOR inhibition induces upstream receptor tyrosine kinase signaling and activates Akt. *Cancer Res*. 2006;66(3):1500-1508.
28. Tamburini J, Chapuis N, Bardet V, et al. Mammalian target of rapamycin (mTOR) inhibition activates phosphatidylinositol 3-kinase/Akt by up-regulating insulin-like growth factor-1 receptor signaling in acute myeloid leukemia: rationale for therapeutic inhibition of both pathways. *Blood*. 2008;111(1):379-382.
29. Yuan J, Mehta PP, Yin MJ, et al. PF-04691502, a potent and selective oral inhibitor of PI3K and mTOR kinases with antitumor activity. *Mol Cancer Ther*. 2011;10(11):2189-2199.
30. Wong CH, Loong HH, Hui CW, et al. Preclinical evaluation of the PI3K-mTOR dual inhibitor PF-04691502 as a novel therapeutic drug in nasopharyngeal carcinoma. *Invest New Drugs*. 2013;31(6):1399-1408.
31. Fang DD, Zhang CC, Gu Y, et al. Antitumor Efficacy of the Dual PI3K/mTOR Inhibitor PF-04691502 in a Human Xenograft Tumor Model Derived from Colorectal Cancer Stem Cells Harboring a Mutation. *PLoS One*. 2013;8(6):e67258.
32. Simmons BH, Lee JH, Lalwani K, et al. Combination of a MEK inhibitor at sub-MTD with a PI3K/mTOR inhibitor significantly suppresses growth of lung adenocarcinoma tumors in Kras(G12D-LSL) mice. *Cancer Chemother Pharmacol*. 2012;70(2):213-220.
33. Wang FZ, Peng J, Yang NN, et al. PF-04691502 triggers cell cycle arrest, apoptosis and inhibits the angiogenesis in hepatocellular carcinoma cells. *Toxicol Lett*. 2013;220(2):150-156.
34. Britten CD, Adjei AA, Millham R, et al. Phase I study of PF-04691502, a small-molecule, oral, dual inhibitor of PI3K and mTOR, in patients with advanced cancer. *Invest New Drugs*. 2014;32(3):510-517.
35. Hallek M, Cheson BD, Catovsky D, et al. Guidelines for the diagnosis and treatment of chronic lymphocytic leukemia: a report from the International Workshop on Chronic Lymphocytic Leukemia updating the National Cancer Institute-Working Group 1996 guidelines. *Blood*. 2008;111(12):5446-5456.
36. Mockridge CI, Potter KN, Wheatley I, Neville LA, Packham G, Stevenson FK. Reversible anergy of sIgM-mediated signaling in the two subsets of CLL defined by VH-gene mutational status. *Blood*. 2007;109(10):4424-4431.
37. Steele AJ, Prentice AG, Hoffbrand AV, et al. 2-Phenylacetylenesulfonamide (PAS) induces p53-independent apoptotic killing of B-chronic lymphocytic leukemia (CLL) cells. *Blood*. 2009;114(6):1217-1225.

38. Steele AJ, Prentice AG, Hoffbrand AV, et al. p53-mediated apoptosis of CLL cells: evidence for a transcription-independent mechanism. *Blood*. 2008;112(9):3827-3834.
39. Steele AJ, Prentice AG, Cwynarski K, et al. The JAK3-selective inhibitor PF-956980 reverses the resistance to cytotoxic agents induced by interleukin-4 treatment of chronic lymphocytic leukemia cells: potential for reversal of cytoprotection by the microenvironment. *Blood*. 2010;116(22):4569-4577.
40. Stevenson FK, Krysov S, Davies AJ, Steele AJ, Packham G. B-cell receptor signaling in chronic lymphocytic leukemia. *Blood*. 2011;118(16):4313-4320.
41. Krysov S, Steele AJ, Coelho V, et al. Stimulation of surface IgM of chronic lymphocytic leukemia cells induces an unfolded protein response dependent on BTK and SYK. *Blood*. 2014;124(20):3101-3109.
42. Herman SE, Gordon AL, Hertlein E, et al. Bruton tyrosine kinase represents a promising therapeutic target for treatment of chronic lymphocytic leukemia and is effectively targeted by PCI-32765. *Blood*. 2011;117(23):6287-6296.
43. Iyengar S, Clear A, Bodor C, et al. P110alpha-mediated constitutive PI3K signaling limits the efficacy of p110delta-selective inhibition in mantle cell lymphoma, particularly with multiple relapse. *Blood*. 2013;121(12):2274-2284.
44. Dong S, Guinn D, Dubovsky JA, et al. IPI-145 antagonizes intrinsic and extrinsic survival signals in chronic lymphocytic leukemia cells. *Blood*. 2014;124(24):3583-3586.
45. Amrein L, Shawi M, Grenier J, Aloyz R, Panasci L. The phosphatidylinositol-3 kinase I inhibitor BKM120 induces cell death in B-chronic lymphocytic leukemia cells in vitro. *Int J Cancer*. 2013;133(1):247-252.
46. Foster JG, Blunt MD, Carter E, Ward SG. Inhibition of PI3K signaling spurs new therapeutic opportunities in inflammatory/autoimmune diseases and hematological malignancies. *Pharmacol Rev*. 2012;64(4):1027-1054.
47. Foukas LC, Bilanges B, Bettedi L, et al. Long-term p110alpha PI3K inactivation exerts a beneficial effect on metabolism. *EMBO Mol Med*. 2013;5(4):563-571.
48. Herishanu Y, Perez-Galan P, Liu D, et al. The lymph node microenvironment promotes B-cell receptor signaling, NF-kappaB activation, and tumor proliferation in chronic lymphocytic leukemia. *Blood*. 2011;117(2):563-574.
49. Burger JA, Tsukada N, Burger M, Zvaifler NJ, Dell'Aquila M, Kipps TJ. Blood-derived nurse-like cells protect chronic lymphocytic leukemia B cells from spontaneous apoptosis through stromal cell-derived factor-1. *Blood*. 2000;96(8):2655-2663.
50. Wodarz D, Garg N, Komarova NL, et al. Kinetics of CLL cells in tissues and blood during therapy with the BTK inhibitor ibrutinib. *Blood*. 2014;123(26):4132-4135.
51. Smit LA, Hallaert DY, Spijker R, et al. Differential Noxa/Mcl-1 balance in peripheral versus lymph node chronic lymphocytic leukemia cells correlates with survival capacity. *Blood*. 2007;109(4):1660-1668.

FIGURE LEGENDS

Figure 1. Inhibition of mTOR augments AKT signaling in CLL which can be overcome by a dual PI3K/mTOR inhibitor. (A) CLL cells were pre-treated with Everolimus (1 μM) or PF-04691502 (1 μM) for 2.5 hours prior to treatment with soluble anti-IgM (IgM) for 15 minutes. Immunoblotting was performed for phosphorylated AKT ($pAKT^{S473}$), S6 kinase ($pS6K^{T389}$) and S6 (pS6 ribsosomal $subunit^{S235/236}$). Bcl-2 was used as a loading control. Graphs (B-E) represent the fold change in $pAKT^{S473}$, $pS6K^{T389}$, $pS6^{S235/236}$ and AKT^{T308} compared to the untreated basal control following the various treatments described above (n=7, 6, 7 and 5 respectively). * represents $p<0.05$. Error bars represent SEM.

Figure 2. PF-04691502 reduces cell viability of CLL cells independently of prognostic markers. (A) CLL samples (n=25) and normal B ($CD19^+$) and T cells ($CD3^+$) (n=5) were treated in the presence or absence of PF-04691502 (0.0049-40μM) for 24 hours. Cell viability was calculated using AnnexinV/PI assays and measured by flow cytometry. For comparison a proportion of the same CLL samples were treated with idelalisib (0.0049-40μM) (n=12). (B) CLL samples (n=6) were treated with PF-04691502 (0.0025-2.5μM) for 24-72h in a small cohort of 6 patients (3 low IC_{50} and 3 high IC_{50} at 24h). (C-E) Correlation of the response to PF-04691502 with prognostic markers IGHV (n=21), ZAP70 (n=23) and CD38 (n=23). Error bars represent SEM.

Figure 3. PF-04691502 induces the intrinsic apoptosis pathway following PI3K/mTOR pathway inhibition. Immunoblotting was utilised to show (A) Expression of the Bcl-2 family of pro-apoptotic proteins namely Noxa and Puma in resting non-activated cells. $pAKT^{S473}$ and $pS6K^{T389}$ were used to confirm PF-04691502 treatment (18h) had inhibited the PI3K/mTOR pathway. HSC70 was the loading control. The figure is representative of 9 independent experiments. (B) BAX conformational change was investigated in the presence or absence of PF-04691502, immunoprecipitation with the BAX 6A7 was performed as described (Supplementary methods). IgH and IgL were included to confirm identical quantities of antibody were used for the immunoprecipitation. Blot is representative of 4 independent experiments. (C) Cleavage of caspase-3 and its substrate PARP (marker of apoptosis), representative blot of 10 independent experiments. (D) CLL samples (n=7) were treated with PF-04691502 as above but with or without the pan-caspase inhibitor ZVAD.fmk and analysed by flow cytometry for Annexin V/PI negativity. (E) Stromal fibroblasts (HFFF2) were co-cultured with CLL cells and the whole well treated in the presence or absence of continuous PF-04691502 (2.5μM) for 24h. CLL cells were removed by pipetting (Supplementary Figure 3D) or scraping (Figure 3E) and cell viability analysed using Annexin V/PI analysis by flow cytometry (n=7). (F) The assay was performed as (E) except that the CLL cells were pre-treated for 1 hours with PF-04691502 prior to drug washed out and the treated CLL cells were plated into wells containing stromal fibroblasts (n=7). Error bars represent SEM. (Method in supplementary data). No difference was observed between scraping all cells or washing off only the CLL cells (compare Figure 3E and Supplementary Figure 3D).

Figure 4. PF-04691502 inhibits anti-IgM induced signaling

CLL cells were treated with (A) soluble anti-IgM (n=9) and (B) immobilised anti-IgM beads (n=5) prior to evaluation of downstream signalling in the presence and absence of PF-04691502 (0.0025-2.5μM) by immunoblot analysis. Representative cases are shown. CLL cells were treated for an hour with PF-04691502 prior to soluble/immobilised anti-IgM addition. $pAKT^{T308}$ and $pS6K^{T389}$ were used as markers of PI3K signalling, $pAKT^{S473}$ and $pS6^{S235/236}$ were used as markers of mTOR signalling and $pERK^{T202/Y204}$ was used as a marker of MAPK signalling.

Figure 5. PF-04691502 inhibits CXCL12 signalling and subsequent migration
(A) CLL cells were treated with 200ng/ml CXCL12 for the times indicated in the presence or absence of PF-04691502 (0.25-2.5μM). PF-04691502 was added 30 minutes prior to the addition of CXCL12. Immunoblotting was performed $pAKT^{S473}$, $pS6K^{T389}$, $pS6^{S235/236}$, $pERK^{T202/Y204}$, total proteins and the loading control Bcl-2 were investigated, immunoblot representative of 6 independent experiments. (B) Using a transwell migration assay we evaluated the migration of CLL cells towards 200ng/ml CXCL12 in the presence or absence of PF-04691502 (1.25-2.5μM). Flow cytometry was used to count the number of cells which had passed through the transwell filter (n=5). Error bars represent SEM. (Method in supplementary data).

Figure 6. PF-04691502 inhibits anti-IgM and CXCL12 induced signalling in Eμ-TCL-1 murine cells.
Eμ-TCL-1 cells were removed from mice and grown *in vitro*. Eμ-TCL-1 cells were treated with (A) anti-IgM (5-15mins) or (B) 200ng/ml CXCL12 in the presence or absence of PF-04691502 (0.0025-2.5μM) and the effects on downstream signalling ($pAKT^{T308}$, $pAKT^{S473}$, $pS6K^{T389}$, $pS6^{S235/236}$ and $pERK^{T202/Y204}$) investigated by immunoblotting. HSC70 was used as a loading control. (C) Viability of Eμ-TCL-1 cells by PF-04691502 was evaluated by AnnexinV/PI assays and represented as percentage viable cells. (D) Migration was performed as previously described in Figure 5B. Error bars represent SEM.

Figure 7. The effect of PF-04691502 in the Eμ-TCL-1 mouse model
Mice inoculated with Eμ-TCL-1 tumor cells were treated by oral gavage with 5 or 10mg/kg/d PF-04691502 or placebo control over 14 days of continual treatment once the emergence of a leukemic phase occurred at day 21 (depicted by the arrow). (A) Peripheral leukemic ($CD5^+CD220^+$) cell number was evaluated by flow cytometry in the presence of PF-04691502 or the vehicle control. (B) Illustration of the spleen sizes from mice treated with 10mg/kg/day PF-04691502 or vehicle control compared to the WT mouse C57BL/6. (C) Represents the spleen weights from (B). (D) Leukemic cell number was also investigated in various organs including spleens (SPL), lymph nodes (LN) and bone marrow (BM) following treatment with PF-04691502 or the vehicle control. Error bars represent SEM.

Figure 1.

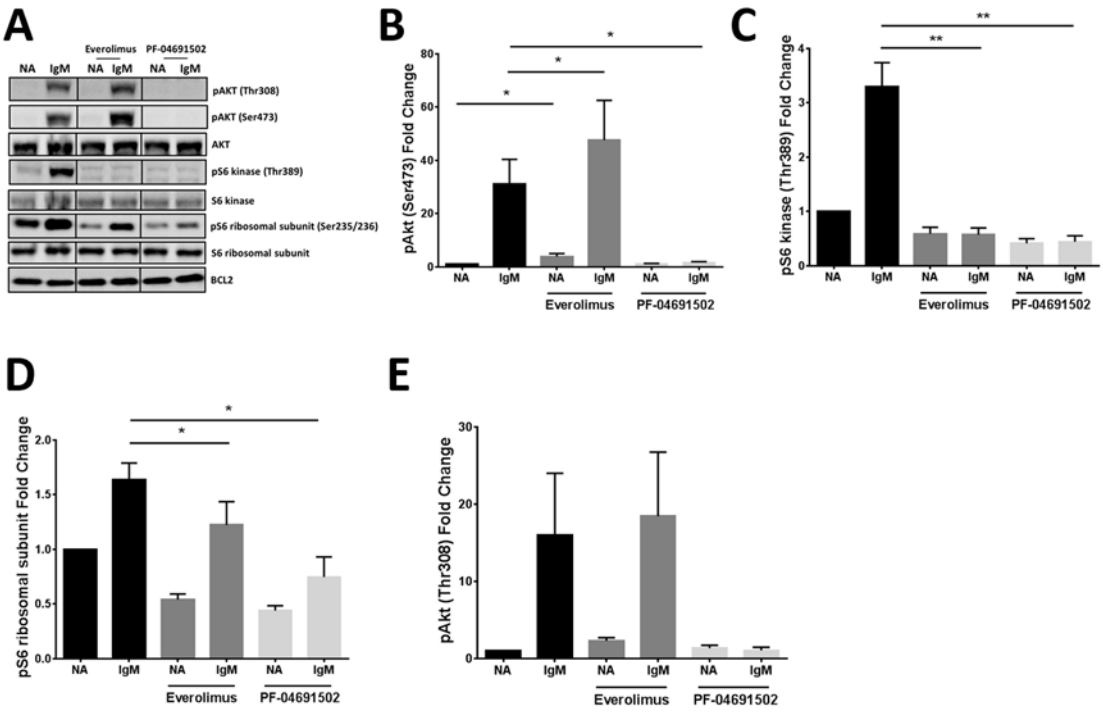
A
Everolimus
PF-04691502
NA IgM NA IgM NA IgM
pAKT (Thr308)
pAKT (Ser473)
AKT
pS6 kinase (Thr389)
S6 kinase
pS6 ribosomal subunit (Ser235/236)
S6 ribosomal subunit
BCL2
B
pAkt (Ser473) Fold Change
NA IgM NA IgM NA IgM
Everolimus
PF-04691502
C
pS6 kinase (Thr389) Fold Change
NA IgM NA IgM NA IgM
Everolimus
PF-04691502
D
pS6 ribosomal subunit Fold Change
NA IgM NA IgM NA IgM
Everolimus
PF-04691502
E
pAkt (Thr308) Fold Change
NA IgM NA IgM NA IgM
Everolimus
PF-04691502

Figure 2.

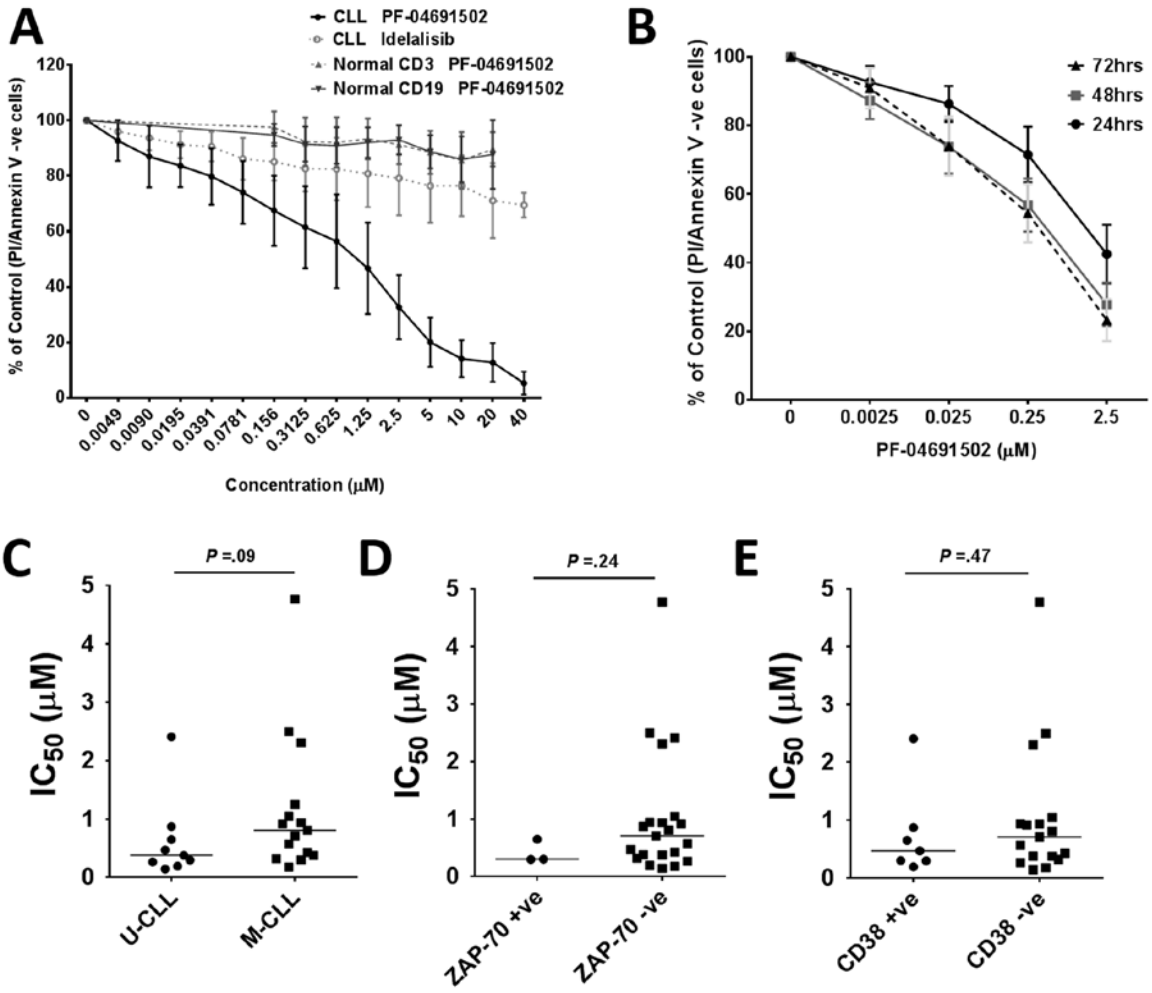
A
CLL PF-04691502
CLL Idelalisib
Normal CD3 PF-04691502
Normal CD19 PF-04691502
% of Control (PI/Annexin V -ve cells)
Concentration (μM)
B
72hrs
48hrs
24hrs
% of Control (PI/Annexin V -ve cells)
PF-04691502 (μM)
C
P =.09
IC50 (μM)
U-CLL
M-CLL
D
P =.24
IC50 (μM)
ZAP-70 +ve
ZAP-70 -ve
E
P =.47
IC50 (μM)
CD38 +ve
CD38 -ve

Figure 3.

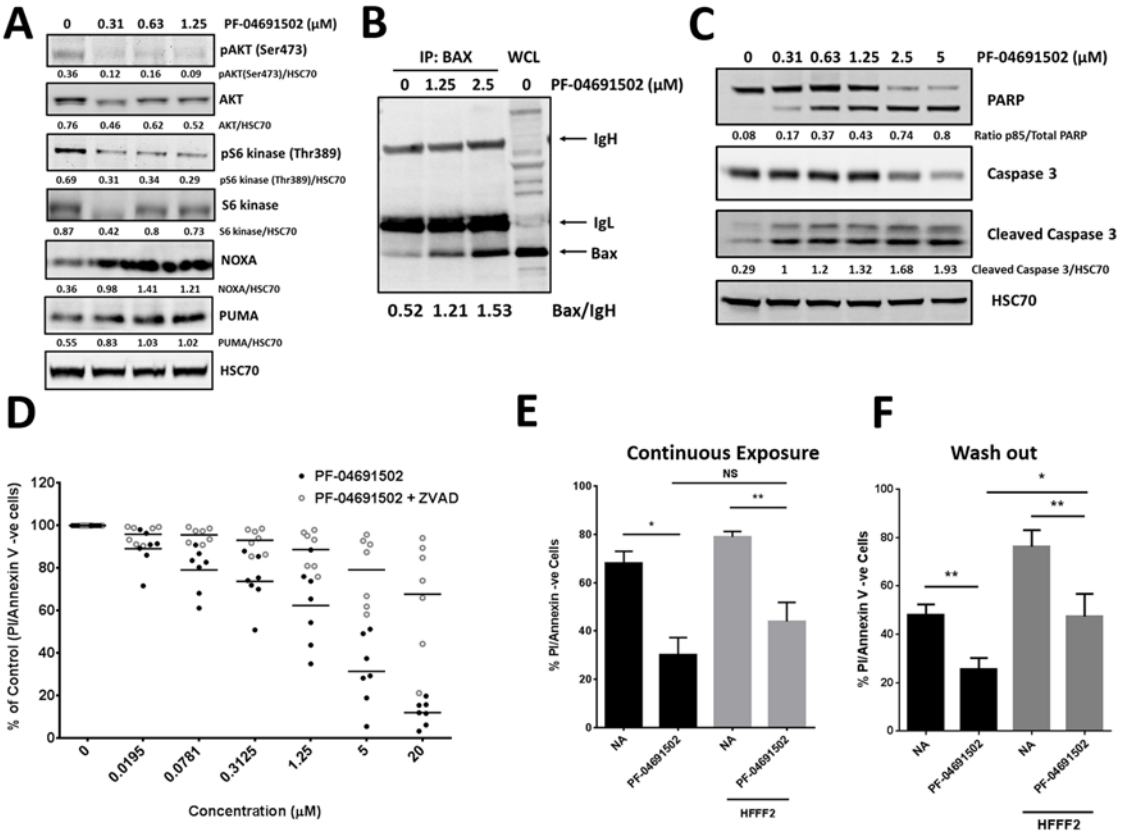
A
0 0.31 0.63 1.25 PF-04691502 (μM)
pAKT (Ser473)
0.36 0.12 0.16 0.09 pAKT(Ser473)/HSC70
AKT
0.76 0.46 0.62 0.52 AKT/HSC70
pS6 kinase (Thr389)
0.69 0.31 0.34 0.29 pS6 kinase (Thr389)/HSC70
S6 kinase
0.87 0.42 0.8 0.73 S6 kinase/HSC70
NOXA
0.36 0.98 1.41 1.21 NOXA/HSC70
PUMA
0.55 0.83 1.03 1.02 PUMA/HSC70
HSC70
B
IP: BAX
WCL
0 1.25 2.5 0 PF-04691502 (μM)
IgH
IgL
Bax
0.52 1.21 1.53 Bax/IgH
C
0 0.31 0.63 1.25 2.5 5 PF-04691502 (μM)
PARP
0.08 0.17 0.37 0.43 0.74 0.8 Ratio p85/Total PARP
Caspase 3
Cleaved Caspase 3
0.29 1 1.2 1.32 1.68 1.93 Cleaved Caspase 3/HSC70
HSC70
D
PF-04691502
PF-04691502 + ZVAD
% of Control (PI/Annexin V -ve cells)
Concentration (μM)
0 0.0195 0.0781 0.3125 1.25 5 20
E
Continuous Exposure
NS
% PI/Annexin -ve Cells
NA PF-04691502 NA PF-04691502
HFFF2
F
Wash out
% PI/Annexin V -ve Cells
NA PF-04691502 NA PF-04691502
HFFF2

Figure 4.

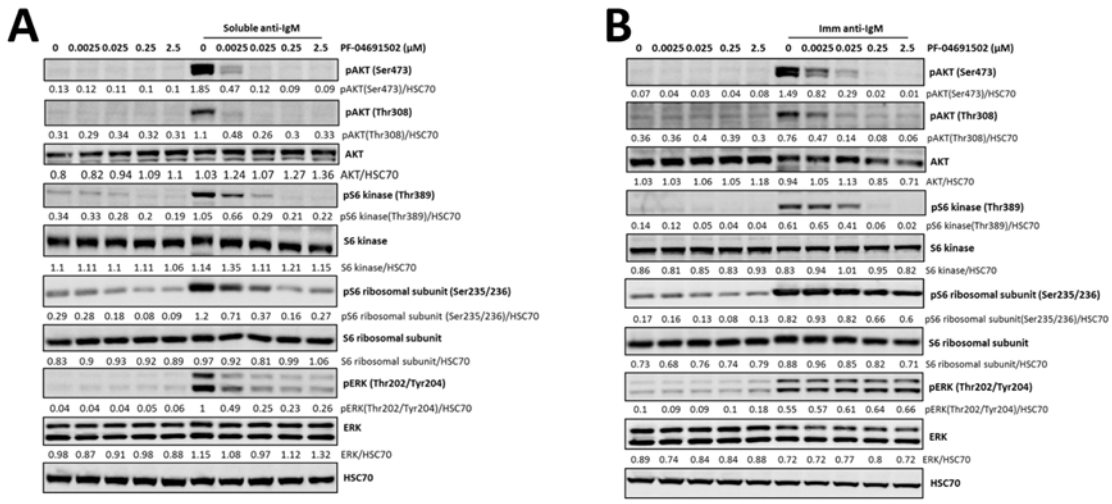
A
Soluble anti-IgM
0 0.0025 0.025 0.25 2.5 0 0.0025 0.025 0.25 2.5 PF-04691502 (μM)
pAKT (Ser473)
0.13 0.12 0.11 0.1 0.1 1.85 0.47 0.12 0.09 0.09 pAKT(Ser473)/HSC70
pAKT (Thr308)
0.31 0.29 0.34 0.32 0.31 1.1 0.48 0.26 0.3 0.33 pAKT(Thr308)/HSC70
AKT
0.8 0.82 0.94 1.09 1.1 1.03 1.24 1.07 1.27 1.36 AKT/HSC70
pS6 kinase (Thr389)
0.34 0.33 0.28 0.2 0.19 1.05 0.66 0.29 0.21 0.22 pS6 kinase(Thr389)/HSC70
S6 kinase
1.1 1.11 1.1 1.11 1.06 1.14 1.35 1.11 1.21 1.15 S6 kinase/HSC70
pS6 ribosomal subunit (Ser235/236)
0.29 0.28 0.18 0.08 0.09 1.2 0.71 0.37 0.16 0.27 pS6 ribosomal subunit (Ser235/236)/HSC70
S6 ribosomal subunit
0.83 0.9 0.93 0.92 0.89 0.97 0.92 0.81 0.99 1.06 S6 ribosomal subunit/HSC70
pERK (Thr202/Tyr204)
0.04 0.04 0.04 0.05 0.06 1 0.49 0.25 0.23 0.26 pERK(Thr202/Tyr204)/HSC70
ERK
0.98 0.87 0.91 0.98 0.88 1.15 1.08 0.97 1.12 1.32 ERK/HSC70
HSC70
B
Imm anti-IgM
0 0.0025 0.025 0.25 2.5 0 0.0025 0.025 0.25 2.5 PF-04691502 (μM)
pAKT (Ser473)
0.07 0.04 0.03 0.04 0.08 1.49 0.82 0.29 0.02 0.01 pAKT(Ser473)/HSC70
pAKT (Thr308)
0.36 0.36 0.4 0.39 0.3 0.76 0.47 0.14 0.08 0.06 pAKT(Thr308)/HSC70
AKT
1.03 1.03 1.06 1.05 1.18 0.94 1.05 1.13 0.85 0.71 AKT/HSC70
pS6 kinase (Thr389)
0.14 0.12 0.05 0.04 0.04 0.61 0.65 0.41 0.06 0.02 pS6 kinase(Thr389)/HSC70
S6 kinase
0.86 0.81 0.85 0.83 0.93 0.83 0.94 1.01 0.95 0.82 S6 kinase/HSC70
pS6 ribosomal subunit (Ser235/236)
0.17 0.16 0.13 0.08 0.13 0.82 0.93 0.82 0.66 0.6 pS6 ribosomal subunit(Ser235/236)/HSC70
S6 ribosomal subunit
0.73 0.68 0.76 0.74 0.79 0.88 0.96 0.85 0.82 0.71 S6 ribosomal subunit/HSC70
pERK (Thr202/Tyr204)
0.1 0.09 0.09 0.1 0.18 0.55 0.57 0.61 0.64 0.66 pERK(Thr202/Tyr204)/HSC70
ERK
0.89 0.74 0.84 0.84 0.88 0.72 0.72 0.77 0.8 0.72 ERK/HSC70
HSC70

Figure 5.

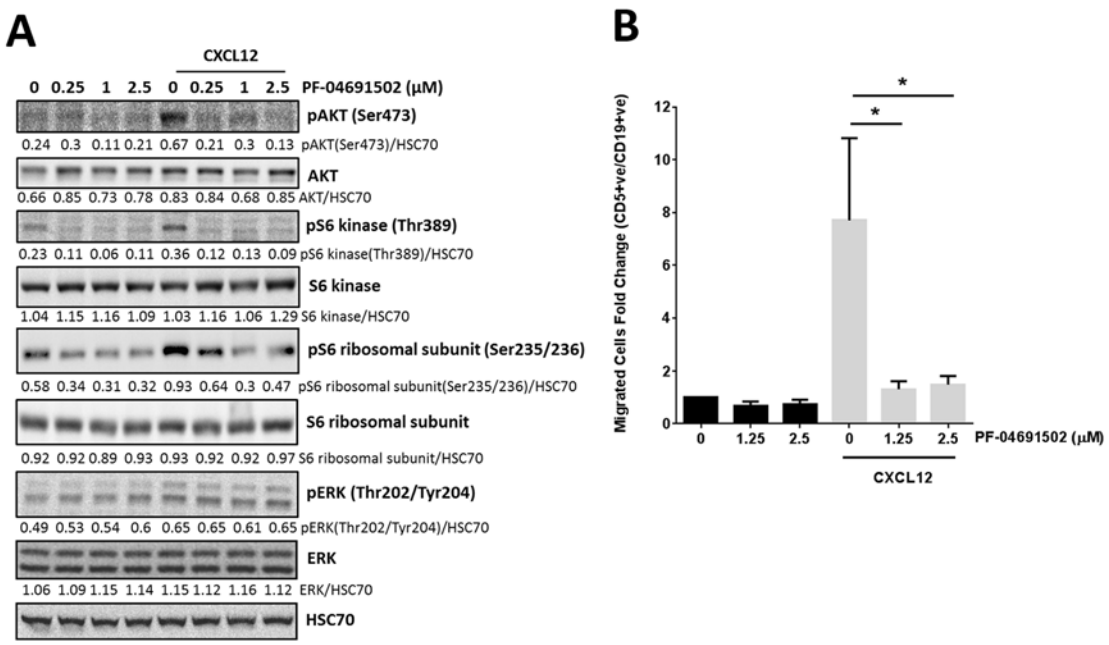
A
CXCL12
0 0.25 1 2.5 0 0.25 1 2.5 PF-04691502 (μM)
pAKT (Ser473)
0.24 0.3 0.11 0.21 0.67 0.21 0.3 0.13 pAKT(Ser473)/HSC70
AKT
0.66 0.85 0.73 0.78 0.83 0.84 0.68 0.85 AKT/HSC70
pS6 kinase (Thr389)
0.23 0.11 0.06 0.11 0.36 0.12 0.13 0.09 pS6 kinase(Thr389)/HSC70
S6 kinase
1.04 1.15 1.16 1.09 1.03 1.16 1.06 1.29 S6 kinase/HSC70
pS6 ribosomal subunit (Ser235/236)
0.58 0.34 0.31 0.32 0.93 0.64 0.3 0.47 pS6 ribosomal subunit(Ser235/236)/HSC70
S6 ribosomal subunit
0.92 0.92 0.89 0.93 0.93 0.92 0.92 0.97 S6 ribosomal subunit/HSC70
pERK (Thr202/Tyr204)
0.49 0.53 0.54 0.6 0.65 0.65 0.61 0.65 pERK(Thr202/Tyr204)/HSC70
ERK
1.06 1.09 1.15 1.14 1.15 1.12 1.16 1.12 ERK/HSC70
HSC70
B
Migrated Cell's Fold Change (CD5+ve/CD19+ve)
0
2
4
6
8
10
12
*
*
0 1.25 2.5 0 1.25 2.5 PF-04691502 (μM)
CXCL12

Figure 6.

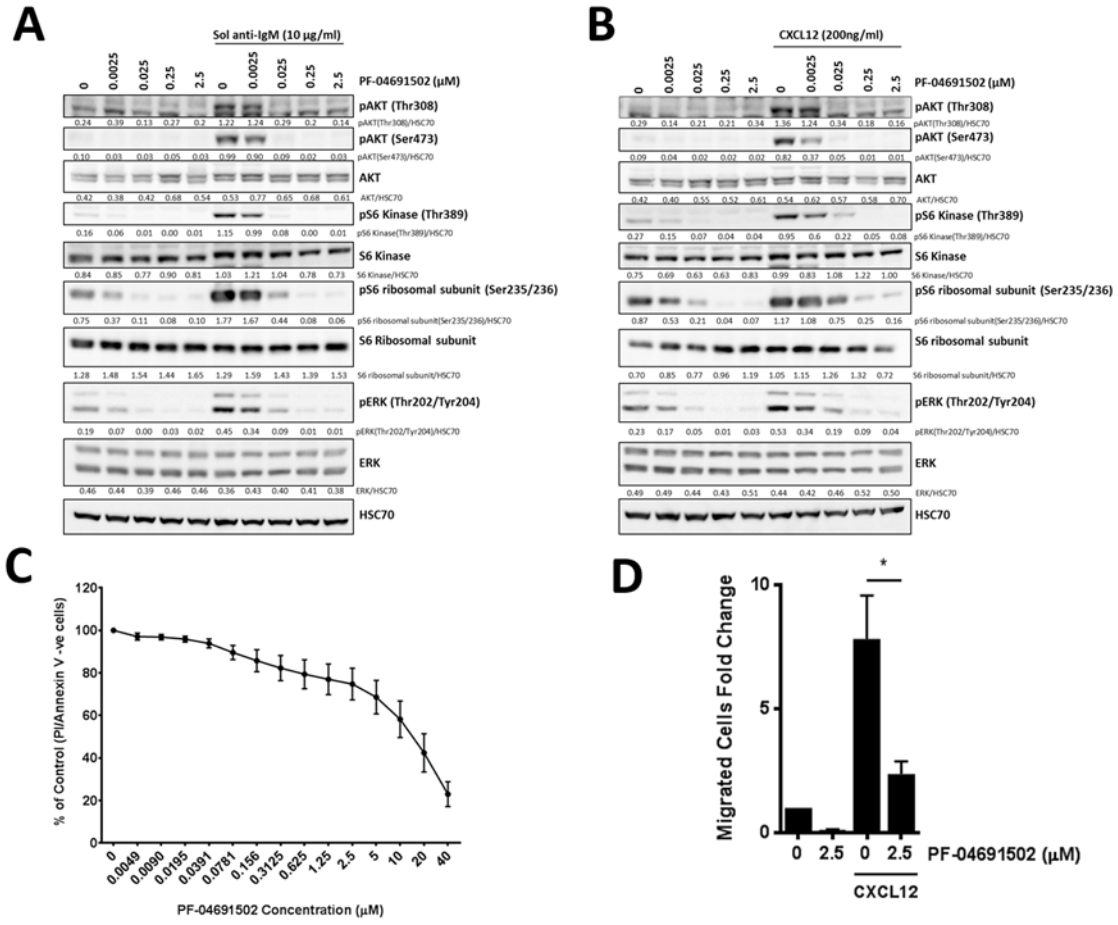
A
Sol anti-IgM (10 µg/ml)
0 0.0025 0.025 0.25 2.5 0 0.0025 0.025 0.25 2.5
PF-04691502 (µM)
pAKT (Thr308)
pAKT (Ser473)
AKT
pS6 Kinase (Thr389)
S6 Kinase
pS6 ribosomal subunit (Ser235/236)
S6 Ribosomal subunit
pERK (Thr202/Tyr204)
ERK
HSC70
B
CXCL12 (200ng/ml)
0 0.0025 0.025 0.25 2.5 0 0.0025 0.025 0.25 2.5
PF-04691502 (µM)
pAKT (Thr308)
pAKT (Ser473)
AKT
pS6 Kinase (Thr389)
S6 Kinase
pS6 ribosomal subunit (Ser235/236)
S6 ribosomal subunit
pERK (Thr202/Tyr204)
ERK
HSC70
C
% of Control (PI/Annexin V -ve cells)
PF-04691502 Concentration (µM)
D
Migrated Cells Fold Change
PF-04691502 (µM)
CXCL12

Figure 7.

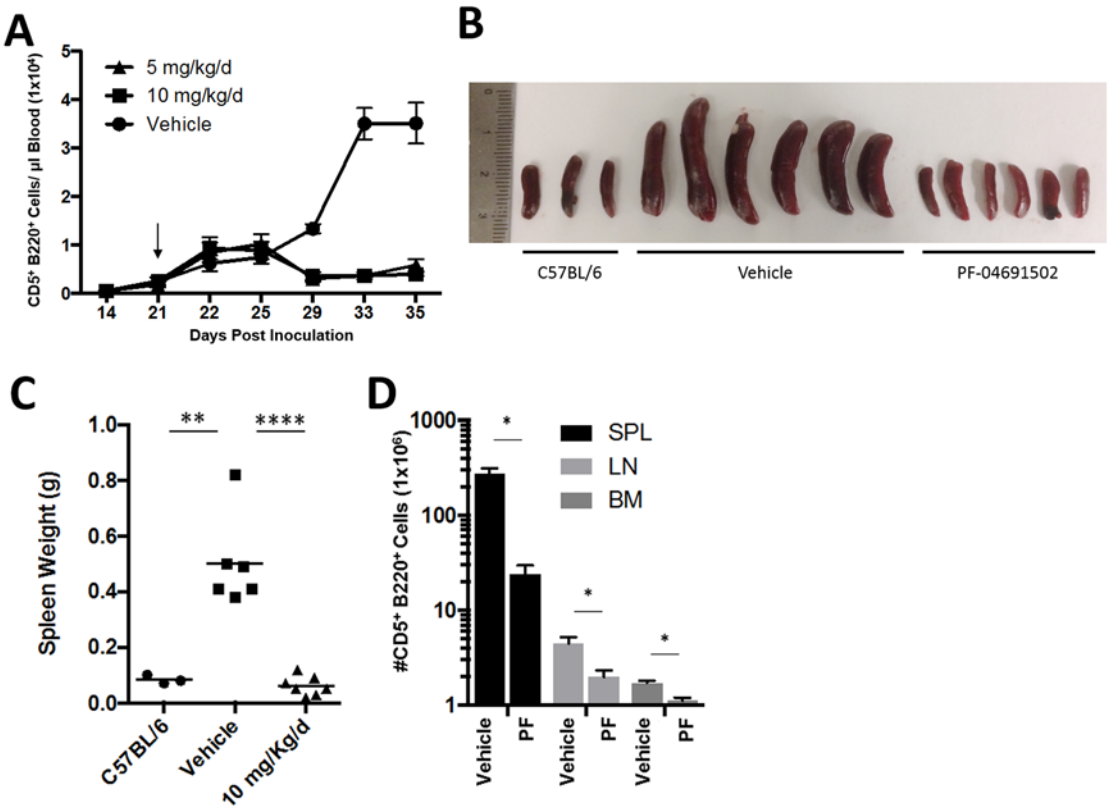
A
5 mg/kg/d
10 mg/kg/d
Vehicle
CD5+ B220+ Cells/ µl Blood (1x10⁴)
Days Post Inoculation
B
C57BL/6
Vehicle
PF-04691502
C
Spleen Weight (g)
**
****
C57BL/6
Vehicle
10 mg/Kg/d
D
#CD5+ B220+ Cells (1x10⁶)
SPL
LN
BM
Vehicle
PF